Equilibration Scales in Silicic to Intermediate Magmas - Implications for Experimental Studies

Michel Pichavant, Fidel Costa Rodriguez, Alain Burgisser, Bruno Scaillet, Caroline Martel, Stéphane Poussineau

Equilibration Scales in Silicic to Intermediate Magmas—Implications for Experimental Studies

Michel Pichavant[1,*], Fidel Costa[2], Alain Burgisser[1], Bruno Scaillet[1], Caroline Martel[1] and Stéphane Poussineau[1]

[1]Institut des Sciences de la Terre D'orléans (ISTO), UMR 6113 CNRS-INSU, Université d'Orléans, 1A Rue de la Férollerie, 45071, Orléans Cedex 02, France
[2]CSIC, Institut de Ciènces de la Terra 'Jaume Almera', Lluis Solé I Sabaris S/N, 08028 Barcelona, Spain

ABSTRACT

Experimental phase equilibrium studies are increasingly being used for the determination of intensive variables (P, T, fH_2O, fO_2) in silicic to intermediate magmas. In contrast, silicic igneous bodies are now perceived as open, periodically recharged, systems involving only limited chemical equilibration. Thus, the use of laboratory-determined crystal–liquid equilibrium data needs clarification. Here we review the field, petrological and geochemical evidence concerning states and scales of chemical equilibrium in silicic magma bodies. It is concluded that total chemical equilibrium is generally not the rule. However, a subsystem in local equilibrium (the reactive magma) can be identified. Equilibration scales in silicic magmas are rate-limited either by diffusive flux in crystals (DICL regime) or by diffusive flux in the melt (MD regime). The recognition that equilibrium in magmas is limited to a reactive subsystem requires phase equilibrium studies to be chemically scaled. Experiments, either of total or partial equilibrium type, should aim at a close reproduction of equilibrium states specific to natural systems. The laboratory reconstruction of the natural equilibrium states guarantees a precise determination of the pre-eruptive parameters and a reliable application of the experimental data to active volcanic systems.

KEY WORDS: *silicic magmas; chemical equilibrium; timescales; experimental studies*

INTRODUCTION

For almost a century, experimental phase equilibrium studies have provided a quantitative basis for understanding magmatic processes. Originally performed on simple synthetic systems (e.g. Mysen, 1989), experimental phase equilibrium studies have shifted to chemically complex compositions containing volatiles and multivalent elements and, thus, have the potential to closely simulate the evolution of silicic to intermediate magmas (e.g. Eggler & Burnham, 1973; Maaloe & Wyllie, 1975; Clemens & Wall, 1981; Naney, 1983; Scaillet *et al.*, 1995). Initially aimed at the formulation of general principles of silicate crystallization and magma differentiation (Bowen, 1913, 1914), phase equilibrium studies are now increasingly being used to determine intensive parameters (*P*, *T*, fH_2O, fO_2) in igneous systems (e.g. Rutherford *et al.*, 1985; Martel *et al.*, 1998; Scaillet & Evans, 1999; Costa *et al.*, 2004). Knowledge of these pre-eruptive parameters is of important practical application for petrological monitoring of active volcanoes, physical modelling of eruptions (Dobran *et al.*, 1994) and for computing compositions of magmatic gases released to the atmosphere (Scaillet & Pichavant, 2003).

The present-day development of phase equilibrium studies has benefited from continuous experimental and analytical improvements. For example, specific methods have been

introduced to promote attainment of crystal–liquid equilibrium in hydrous, SiO_2-rich magmas at relatively low temperatures (e.g. Pichavant, 1987; Holtz *et al*., 1992; Scaillet *et al*., 1995). Therefore, it has now become technically possible to chemically equilibrate a wide range of silicate compositions in the laboratory. However, igneous systems in nature are increasingly appreciated to be out-of-equilibrium and, therefore, the use of laboratory-determined crystal–liquid equilibrium data needs to be rigorously justified.

Experimental petrologists very early on recognized that total equilibrium is not the rule in natural magmas and that, theoretically, cooling rates and reaction kinetics should affect crystallization paths (e.g. Bowen, 1914; Young, 1998). Nevertheless, the application of phase equilibrium studies to igneous rocks has been generally justified (e.g. Schairer, 1957). Similarly, the use of mineral–mineral or mineral–melt geothermobarometers to retrieve intensive variables (e.g. Buddington & Lindsley, 1964; Carmichael *et al*., 1970) and of crystal–liquid partitioning to model magmatic processes (e.g. Gast, 1968; Allègre & Minster, 1978) both rely on the assumption that chemical equilibration occurs, at least locally, in igneous rocks. In contrast, various studies have stressed the importance of magma mixing and mingling, hence of disequilibrium, in igneous systems (e.g. Kuno, 1950; Anderson, 1976; Eichelberger, 1978). The view that igneous bodies are open, periodically recharged systems involving limited equilibration has progressively gained acceptance. More recently, the development of analytical techniques has extended to small scales the documentation of trace element and isotopic disequilibrium in igneous processes (e.g. Bea, 1996*a*, 1996*b*; Hammouda *et al*., 1996; Davidson & Tepley, 1997; Knesel *et al*., 1999). Therefore, there is an heightened appreciation that chemical equilibrium is not necessarily established in igneous systems.

The trend toward the application of phase equilibria to natural magmas, on one hand, and the recognition that magmas are not necessarily near-equilibrium systems, on the other, call for a methodological clarification. In this paper, we contend that the specifics of natural equilibrium states should be better taken into consideration, and that phase equilibrium experiments should aim at the reproduction of equilibrium states specific to magmatic systems. With this approach, the intensive parameters (P, T, fH_2O, fO_2) to be experimentally constrained can be viewed simply as the variables controlling natural pre-eruptive equilibration. Their reliable determination requires matching between experimental data (phase assemblages, mineral and glass compositions) and natural eruption products (phenocryst assemblages and phenocryst and glass compositions) or, in other words, matching between experimental and natural equilibrium states. To reach this goal, both a precise evaluation of natural equilibrium states and methods that allow these natural equilibrium states to be experimentally adjusted are necessary.

This paper consists of two complementary parts. In the first part, the field, petrological and geochemical evidence concerning states and scales of chemical equilibrium in silicic to intermediate (i.e. andesitic to rhyolitic) magmas is analysed. We argue that total equilibrium is generally not the rule. However, a subsystem in local equilibrium can be identified. A general approach to evaluate natural equilibration scales is outlined and illustrated by several natural examples. In the second part, the implications for experimental studies are considered. Methods allowing natural equilibrium states to be experimentally adjusted are presented and discussed.

STATES OF EQUILIBRIUM IN SILICIC TO INTERMEDIATE MAGMAS

Total chemical equilibrium?

Most silicic to intermediate igneous bodies, especially from convergent plate boundaries, can be viewed as hybrid, periodically recharged open systems that preserve evidence for chemical heterogeneities at various scales (e.g. Eichelberger *et al.*, 2000; Fig. 1). At large to medium scales (from 10^5 down to 10^1 cm), chemically zoned ash-flow sheets (Smith, 1979) and plutons (e.g. Pons *et al.*, 2006), mafic enclaves (Bacon, 1986) and banded rocks (Smith, 1979; Poussineau, 2005), illustrate the existence of compositional heterogeneities associated with magma chamber recharge and evolution (Fig. 1). The origin of these compositional gradients is still debated (e.g. Eichelberger *et al.*, 2000, 2006). Although one should bear in mind that chemically heterogeneous whole-rock compositions do not necessarily imply chemical disequilibrium, the evidence from large to medium scales of observation consistently indicates at best limited (or incomplete) chemical equilibration in magma bodies (Eichelberger *et al.*, 2000, 2006). Recent models favouring magma reservoirs as the product of amalgamation of small discrete magma batches (Glazner *et al.*, 2004; Annen *et al.*, 2006) imply scales of chemical equilibration necessarily smaller than in the case of a once molten single large body.

Probably the best evidence for the lack of total chemical equilibration (Table 1) in magmas comes from small-scale (10^0 down to 10^{-4} cm) petrographical, mineralogical and geochemical observations (Fig. 1b and c). As a rule, crystal populations in silicic to intermediate magmas, especially from convergent plate boundaries, are heterogeneous and may include cognate phenocrysts, phenocrysts inherited from a previous crystallization episode (inherited phenocrysts) and xenocrysts. Isotopic fingerprinting techniques now unambiguously demonstrate the mixed origin of individual crystals (e.g. Cioni *et al.*, 1995; Davidson & Tepley, 1997; Knesel *et al.*, 1999). Disequilibrium phenocryst assemblages comprising, for example, calcic plagioclase, Al-rich amphibole, Mg-rich olivine and Cr-spinel coexisting with sodic plagioclase, Al-poor amphibole, quartz and a rhyolitic interstitial glass frequently occur, sometimes in the same rock (e.g. Feeley *et al.*, 1996; Clynne, 1999; Costa & Singer, 2002). Mantling and/or resorption textures on amphibole or biotite (Rutherford & Hill, 1993; Fougnot *et al.*, 1996) indicate reaction relationships, hence disequilibrium, between phenocrysts and melt. Fe–Mg exchange equilibrium may not be established, as shown by the occurrence of homogeneous (i.e. constant Fe/Mg ratio) cummingtonite and biotite coexisting with grossly heterogeneous orthopyroxene and hornblende phenocrysts (e.g. Schmitz & Smith, 2004). Compositionally zoned crystals imply growth under variable compositions and pre-eruptive P–T–$f\mathrm{H_2O}$–$f\mathrm{O_2}$ conditions without subsequent re-equilibration. For plagioclase phenocrysts (e.g. Singer *et al.*, 1995; Pichavant *et al.*, 2002; Fig. 1c), the kinetics of CaAl–NaSi atomic diffusion is extremely slow (Tsuchiyama, 1985), and diffusive chemical equilibration for crystals 10^{-1} to 10^0 cm in size may require durations longer than typical lifetimes of magma chambers (see below). Therefore, total equilibrium is generally not the rule in silicic to intermediate magmas.

Evidence for local equilibrium

Like any natural system governed by the laws of thermodynamics, magmas spontaneously tend to evolve toward chemical equilibrium, to an extent that depends on timescales of magmatic processes and on reaction kinetics. As for metamorphic systems (Thompson, 1959), it may be postulated that local equilibrium (Table 1), that is, the existence of a subsystem of limited spatial extent that achieves chemical equilibrium, applies to silicic to intermediate magmas. Although commonly assumed, but rarely explicitly justified, local equilibrium can be tested by a variety of approaches, some of which are outlined below.

The most straightforward method is to compare natural phase assemblages and compositions with data from phase equilibrium studies. For example, compositions along electron microprobe traverses in phenocrysts from Mt. Pelée and Volcán San Pedro eruptive products are compared with results from phase equilibrium experiments performed on samples representative of each magma (Fig. 2). Assemblages and rim compositions of the main phenocrysts phases are simultaneously reproduced or bracketed by experimental charges (Fig. 2). Al_2O_3 and TiO_2 (not shown) concentrations in amphibole phenocrysts from the San Pedro dacite are also experimentally bracketed. SiO_2 contents of natural glasses and of experimental glasses in these critical charges overlap (Fig. 2). Thus, prior to eruption, coexisting mineral and melt phases in these two magmas were at chemical equilibrium. This is the condition necessary for the pre-eruptive parameters of each reservoir to be determined from the P–T–$f$$H_2O$–$f$$O_2$ of the respective critical charges (for details, see Martel *et al.*, 1999; Costa *et al.*, 2004). It should be noted that plagioclase core compositions are not reproduced by the experiments (Fig. 2). This implies that chemical equilibrium with the liquid is restricted to plagioclase rims. Consequently, in the two examples considered, total equilibrium is not established at the scale of the entire magma, yet a chemically equilibrated subsystem can be identified.

The preceding approach is the most general to test for chemical equilibrium between coexisting magmatic phases, as it allows the assemblage and composition of all phases present to be checked. However, equilibrium data for the magma of interest must be available, either from experiments or from thermodynamic models (see below). Other, less general methods involve testing the compositions of a subset of magmatic phases, such as glasses or selected phenocrysts. For example, natural glasses from Mt. St. Helens eruption products follow major element compositional trends similar to those of experimental liquids from phase equilibrium studies (Blundy & Cashman, 2001), suggesting that their compositions are controlled by crystal–liquid equilibrium relations. Models of element partitioning between coexisting phases also provide a test. The demonstration that Fe–Ti oxide and feldspar phenocryst pairs satisfy element partitioning models in a large number of magmatic systems (Bacon & Hirschmann, 1988; Fuhrman & Lindsley, 1988) constitutes positive evidence for local equilibrium, at least between the respective phenocrysts. Finally, thermobarometric calculations on assemblages of coexisting phenocrysts or phenocrysts plus melt can also be used to check for chemical equilibration in magmas. The fact that several independent thermometers and barometers yield a narrow range of P–T conditions (e.g. Manley & Bacon, 2000) is strong evidence for pre-eruptive equilibration between the phases used in the calculations. In the same way, the Al-in-hornblende barometer for estimating pressures of crystallization of intermediate calc-alkaline plutons is based on the chemical equilibration, either totally or partially along their rims, of at least nine coexisting phases. The validity of the barometer has been confirmed by comparing pressures derived from experimental calibration and from contact-aureole assemblages (e.g. Schmidt, 1992), thus strongly suggesting that hornblende, melt and the other mineral phases equilibrate until near-solidus conditions. Therefore, we conclude that local equilibrium is the prevailing situation in silicic to intermediate magmas.

EQUILIBRATION SCALES

Equilibration mechanisms

In the context of local equilibrium, the spatial extent of the equilibrated subsystem, or equilibration scale (Table 1), must be defined. For silicic magmas, equilibration scales may conceivably range from 10^{-4} (interface between phases) to 10^{5} cm (magma body). A first-order appreciation of equilibration scales may be obtained from the analysis of the dispersion

of whole-rock compositions. However, chemical homogeneity at the hand specimen scale (or larger) may mask heterogeneities at smaller scales, as emphasized above. Therefore, investigations at scales as low as 10^{-4} cm are usually necessary.

Magmatic systems may evolve toward chemical equilibrium through a variety of reaction mechanisms, including nucleation and growth of new crystals, dissolution of pre-existing crystals, coupled crystal dissolution and reprecipitation and diffusive equilibration within crystal and melt phases. Vesiculation of gas bubbles also needs to be considered in volatile-bearing systems subjected to pressure gradients. Thus, equilibration scales depend on the kinetics of these individual reaction mechanisms. Rates of crystal growth are essentially controlled by reactions at the crystal–melt interface and by chemical diffusion in the melt (e.g. Kirkpatrick, 1981; Cashman, 1990). Crystal dissolution may be either reactive (i.e. rate-controlled by interface processes) or diffusive (Liang, 1999). In the latter case, it is essentially rate-controlled by diffusion in the melt (Kuo & Kirkpatrick, 1985; Zhang *et al.*, 1989; Liang, 1999), and diffusion in crystals is unimportant (Liang, 2000) unless coupled dissolution–reprecipitation in a finite geometry is specifically considered (Liang, 2003). Rates of bubble growth essentially depend on diffusion in the melt and also on the melt viscosity (e.g. Navon *et al.*, 1998; Martel & Bureau, 2001; Castro *et al.*, 2005). It is worth stressing that the rates of some of the reaction mechanisms above are strongly influenced by the flow regime. Convective crystal dissolution (e.g. Kerr, 1995), which is probably the dominant dissolution mechanism in natural magmas (Liang, 2000), is faster than diffusive dissolution. In the same way, nucleation rates for plagioclase and clinopyroxene are markedly higher in dynamic (e.g. stirred) than in static crystallization experiments (Kouchi *et al.*, 1986). Conversely, processes such as crystal growth or dissolution may promote convection; for example, through the production of boundary melts with densities different from that of the far-field melt. Therefore, for a rigorous evaluation of equilibration rates, a coupled chemical reaction–transport approach (e.g. Lasaga, 1998) is probably necessary.

Despite these complexities, all that is needed for the present discussion is a comparison between the rates of the individual equilibration mechanisms mentioned above. Timescales of chemical diffusion in representative crystals and in hydrous melt, normalized to a diffusion distance of 1 cm, are shown in Fig. 3. Most calculations are for major elements because these are the elements governing phase equilibria. The components selected for the calculations in Fig. 3 (e.g. CaAl–NaSi in plagioclase, Ca in diopside, Fe–Ti in magnetite, SiO_2 and H_2O in hydrous melt) are assumed to be rate-limiting for their respective phase. In other words, equilibration for the other components (either major, minor or trace elements) would take place at rates equal or faster than equilibration for the elements considered in Fig. 3. As an illustration, Mg diffusion is faster than NaSi–CaAl in plagioclase by at least two orders of magnitude (Fig. 3; La Tourette & Wasserburg, 1998; Costa *et al.*, 2003). MgO concentrations in the plagioclase phenocryst from San Pedro (Fig. 4) closely follow the variations in An content (Fig. 3), whereas in the Mt. Pelée phenocryst MgO concentrations are homogeneously distributed in most of the crystal despite strong variations in An content (Fig. 4). Although we recognize that a component-specific treatment would be more rigorous, the approach followed here has the advantage of relative simplicity and is sufficient for our purpose.(opx)$^{Al}{}_{2}{}^{O}{}_{3}$

In Fig. 3, crystalline phases have by far the longest diffusion timescales, implying that diffusion in crystals and diffusion-in-crystal-controlled reprecipitation (Liang, 2003) are the slowest equilibration mechanisms. A large difference in equilibration timescales is apparent between crystalline phases (nearly 10 orders of magnitude between magnetite and zircon), despite the fact that the results for zircon concern a trace element (Pb) that diffuses faster than

tetravalent cations such as Hf, Th and U (Cherniak & Watson, 2003). This stresses the necessity of a phase-by-phase approach, each crystalline phase having a characteristic equilibration scale. In contrast, mechanisms involving diffusive flux in the melt have more grouped timescales, within 3–4 orders of magnitude of each other (Fig. 3). Diffusive equilibration in the hydrous melt, which can also be taken as an order-of-magnitude estimate for the rate of diffusive crystal dissolution (Kuo & Kirkpatrick, 1985; Zhang *et al*., 1989; Liang, 1999), is the third slowest mechanism. There is a large difference between diffusion timescales in crystals and in the hydrous melt: at 900°C, diffusive equilibration (normalized to 1 cm) in plagioclase requires durations around six orders of magnitude longer than in hydrous melt. Compared with diffusive crystal dissolution, convective crystal dissolution is two orders of magnitude faster (Fig. 3). Timescales for bubble growth in low-viscosity melts, estimated from the H_2O diffusion data (Navon *et al*., 1998; Martel & Bureau, 2001; Castro *et al*., 2005), overlap with crystal growth in hydrous melts (Cashman, 1990) and are in the same range as convective crystal dissolution (Fig. 3). These last mechanisms (crystal and bubble growth, convective crystal dissolution) appear to be the fastest.

Equilibration regimes

The analysis above stresses the marked contrast in equilibration rates between mechanisms controlled by diffusive flux in crystals and those controlled by diffusive flux in the melt. Therefore, it is proposed to distinguish between two end-member equilibration regimes in silicic to intermediate magmas: (1) diffusion-in-crystals-limited (DICL); (2) melt-dominated (MD) equilibration regimes.

(1) The common coexistence of a homogeneous interstitial melt with chemically zoned phenocrysts demonstrates that diffusion in crystals and/or diffusion-controlled reprecipitation rate-limit the approach toward equilibrium in many silicic to intermediate magmas. A homogeneous interstitial melt is a sign that there is no diffusive flux in the melt. Because diffusion in crystals is slow (Fig. 3), the DICL regime is necessarily associated with relatively long magmatic timescales, longer than the characteristic timescales for convection in magmas (from days to months from evidence in natural systems). Because diffusive equilibration in crystals is directly linked to magmatic timescales (e.g. Costa *et al*., 2003; Hawkesworth *et al*., 2004), equilibration scales can be calculated from diffusivities if residence times of crystals are known. As an illustration of the approach, equilibration scales are calculated and shown in Fig. 5 for an equilibration regime rate-controlled by diffusion in crystals. Timescales ranging from a few decades, through a few hundred thousand years to 1 Ma, typical of residence times of crystals in intermediate to silicic magma chambers (Costa & Chakraborty, 2004; Hawkesworth *et al*., 2004; Costa & Dungan, 2005), are considered. Magnetite phenocrysts require durations much shorter than 5000 years to homogenize by diffusion (i.e. of the order of 30 years for an equilibration distance of 200 μm; Fig. 5). In contrast, more than 1 Ma is necessary to homogenize plagioclase phenocrysts over distances >1 mm (Fig. 5). Zircon is much slower than plagioclase to homogenize (<10 μm after 1 Ma; Fig. 5). The calculations show that, for a magma chamber having evolved under closed-system and steady-state pre-eruption conditions (900°C) for 5000 years, only plagioclase (and zircon, if present) can preserve out-of-equilibrium compositions. The equilibration scale would thus be essentially limited by the presence of plagioclase phenocrysts (Fig. 6). Examples of such a situation are provided by the Mt. Pelée andesite and the San Pedro dacite, which both have strongly zoned plagioclase phenocrysts coexisting with homogeneous Fe–Ti oxides, orthopyroxene, amphibole and interstitial melt (Fig. 2).

This approach cannot be extrapolated to very short timescales because other faster equilibration mechanisms will become involved. However, for practical purposes, it is worth emphasizing that certain crystalline phases such as magnetite are able to record thermal perturbations of relatively short durations. For example, calculations as in Fig. 5 show that magnetite should re-equilibrate over distances of the order of 10 μm (i.e. detectable with the electron microprobe) after 100 days at 900°C (Nakamura, 1995; Hammer *et al*., 2002; Devine *et al*., 2003).

(2) The occurrence in some magmatic systems of chemically heterogeneous interstitial glasses (see below for illustration and examples) shows that equilibration scales in magmas are not always limited by diffusion in crystals. Heterogeneous interstitial glasses imply the existence of chemical gradients in the melt phase quenched by the eruption. These gradients are the sign that equilibration mechanisms such as convective mixing between melts, chemical diffusion in the melt, crystallization and/or crystal dissolution are taking place, most probably in response to compositional and thermal perturbations of the system (Fig. 6). From Fig. 3, these mechanisms all have relatively short timescales and, therefore, they will not last for very long unless the system is periodically recharged. Because the rates of these reaction mechanisms are strongly influenced by the flow regime (Fig. 3), we view convective motion as being intimately linked with the MD regime. Eventually, once convection has ceased, the chemical gradients in the melt phase will progressively smooth out and the system will enter the DICL equilibration regime until the next recharge of the magma reservoir.

Koyaguchi & Kaneko (2000) have distinguished two stages in the thermal evolution of silicic magma chambers after basalt replenishment, an initial short-duration convective-melting followed by a long-duration conductive cooling stage. During the first stage, melting and crystallization take place rapidly in the presence of a convecting liquid; the second stage corresponds to slow conductive cooling at constant melt fraction (Koyaguchi & Kaneko, 2000). Chemical equilibration during the first stage would thus proceed by reaction mechanisms such as convective mixing between liquids, crystal dissolution and crystallization (i.e. by MD processes), and during the second stage by intracrystalline diffusion at slowly decreasing temperature (i.e. by DICL processes) (Fig. 6). Therefore, the thermal evolution of periodically recharged silicic magma bodies induces mechanisms of chemical equilibration that are in close correspondence to the two end-member regimes identified in this paper. This provides a physical framework for the development of the MD and DICL equilibration regimes in magma chambers.

Natural illustrations and examples

In practice, the evaluation of equilibration scales in natural magmas, which must be based on detailed field studies, requires petrographical, mineralogical and geochemical data at different scales, from the whole-rock hand specimen down to the micrometre. One factor that needs to be assessed first is the major element composition of interstitial glasses. Homogeneous glasses imply crystal-limited equilibration scales, making detailed studies of phenocryst assemblages and zonations in crystals appropriate. Heterogeneous interstitial glasses are the signs of chemical gradients frozen in the melt phase, and it is necessary first to constrain the scale of chemical variability in glasses before attention is turned to crystals.

Homogeneous interstitial glasses are commonly encountered in andesitic–dacitic lavas erupted from central-vent volcanoes. At the whole-rock scale (centimetres to decimetres), these eruption products show restricted chemical variability, apart from the common presence of mafic enclaves. Examples include Mt. Pinatubo 1991 (Scaillet & Evans, 1999), Mt. Pelée

(Martel *et al*., 1998, 2000), Soufrière Hills (Harford *et al*., 2003) and Volcán San Pedro (Costa & Singer, 2002), among others. In this group, the chemical dispersion of interstitial glass composition is typically small (e.g. < 5 wt % SiO_2). No general and systematic variation in glass chemistry, for example with position in the eruptive sequence, is observed. Another important group with homogeneous interstitial glasses comprises evolved compositions (rhyodacites and rhyolites) from zoned magma chambers. Examples include Krakatau 1883 (Mandeville *et al*., 1996), Mt. Mazama 6845 BP (Bacon & Druitt, 1988) and Novarupta 1912 (Coombs & Gardner, 2001; Hammer *et al*., 2002). In all these examples, the equilibration scale is controlled by diffusive equilibration in phenocrysts and by diffusion-in-crystal-controlled reprecipitation (DICL equilibration regime). An extreme case of reduction of the equilibrium scale occurs when phenocrysts are all out of equilibrium with the interstitial melt, as proposed for the recent dacitic eruption of Mt. Unzen (Nakada & Motomura, 1999). Conversely, nearly aphyric and chemically homogeneous magma bodies (e.g. Novarupta 1912 rhyolite, Coombs & Gardner, 2001) probably approach total equilibrium. For higher, more frequent, phenocryst contents, plagioclase limits equilibration scales in many intermediate arc magmas (the situation discussed above and in Figs 2 and 5). The persistence of quartz xenocrysts in andesite (e.g. Hammer *et al*., 2002) may be attributed to the exceptionally sluggish dissolution kinetics of quartz. Quartz dissolution is dominated by interfacial kinetics (Hammouda & Pichavant, 1999) rather than by chemical diffusion in the melt as for most other mineral phases (Kuo & Kirkpatrick, 1985; Zhang *et al*., 1989; Liang, 1999).

Examples of chemically variable interstitial glasses are provided by large-volume caldera-forming zoned eruptions, such as Krakatau 1883, Mt. Mazama 6845 BP, Novarupta 1912 and Laacher See Tephra, among others. The Laacher See Tephra (Wörner & Schmincke, 1984) illustrates the case of interstitial glass compositions varying regularly along with the location in the eruptive sequence. The compositional variations concern the major, but also the minor and the trace elements. For example, CaO decreases and Th increases from around 4 wt % and 10 ppm at the top to 0·4 wt % and 120 ppm at the base of the sequence (Wörner & Schmincke, 1984). Thus, a continuous and progressive chemical zonation of interstitial glasses is established at the scale of the entire magma reservoir (10^4–10^5 cm). At smaller scales (below 10^2–10^3 cm?), the melt phase may be chemically homogeneous although this remains to be confirmed by appropriate studies. In general, the smaller the scale of the chemical homogeneity in glasses, the smaller the equilibration scale.

Glasses in mafic products of the Mt. Mazama 6845 BP, Krakatau 1883 and Novarupta 1912 eruptions systematically exhibit compositional gradients (Bacon & Druitt, 1988; Mandeville *et al*., 1996; Hammer *et al*., 2002). The range of matrix glass SiO_2 contents is 67–74 wt % in the Krakatau 1883 grey dacite (Mandeville *et al*., 1996), 63–72 wt % in the Mt. Mazama 6845 BP andesites and cumulate scoriae (Bacon & Druitt, 1988) and 67–79 wt % in the Novarupta 1912 andesitic to dacitic products (Hammer *et al*., 2002). These glasses are chemically heterogeneous at various scales. The Krakatau 1883 products document chemical zonation in the melt phase at scales as small as $<10^0$ cm (heterogeneity in glass composition at the thin-section scale, Mandeville *et al*., 1996); a compositional gap in melt composition is present (Mandeville *et al*., 1996). These features necessarily imply that compositionally distinct magmatic liquids coexisted over very short timescales in the magma chamber before the eruption. In the Mt. Mazama 6845 BP products, interstitial glass MgO concentrations correlate with Fe–Ti oxide temperatures (Druitt & Bacon, 1989). This implies that Fe–Ti oxides had sufficient time to equilibrate to the locally prevailing temperature and, thus, that the melt phase may be chemically homogeneous over distances $>10^0$–10^1 cm (Fig. 3). In the same way, the variations in glass SiO_2 concentrations at the thin-section scale in the Krakatau 1883

products are superimposed on a longer-scale chemical variation, marked by the correlation between glass SiO_2 concentrations and Fe–Ti oxide temperatures (Mandeville *et al.*, 1996). Therefore, different scales of chemical variability in the melt phase may be juxtaposed. Both the Krakatau and Mazama systems stress the link between MD equilibration mechanisms, compositional zonations in the melt phase and thermal gradients. Systems with zoned interstitial glasses can be viewed as the sum of small individual subsystems, each equilibrated under local conditions of temperature. This stresses the fact that, for such systems, any determined set of pre-eruptive parameters is of local significance only.

In conclusion, the large dispersion of equilibration scales in nature, from $<10^0$ to 10^4–10^5 cm, must be emphasized. It is consistent with the timescales of physical processes that affect silicic magma chambers (Hawkesworth *et al.*, 2004).

THE LOCAL EQUILIBRIUM MODEL

The main conclusions of the analysis above concerning chemical equilibrium in silicic to intermediate magmas can be summarized as follows.

(1) Total chemical equilibrium is generally not the rule, although exceptions approaching this situation probably exist. However, a subsystem in local equilibrium can be typically identified in all natural magmas. The recognition that local equilibrium is the prevailing case validates the use of principles of chemical equilibrium to interpret compositional diversity and heterogeneities at various scales in magmas.

(2) Equilibration scales in magmas are rate-limited either by diffusive flux in crystals (DICL regime) or by diffusive flux in the melt (MD regime). In the former case, equilibration mechanisms are relatively slow and associated with relatively long timescales. In the latter case, relatively short mechanisms, intimately linked with convective motion, are involved. Equilibration scales in the DICL regime can be estimated from data on magmatic timescales and diffusivities in crystals. For the MD regime, the evaluation of equilibration scales requires first that the convective state of the system is specified.

It is proposed to make a formal distinction between two discrete parts in silicic magmas. The *first part* corresponds to the subsystem of defined volume that is at chemical equilibrium, and whose spatial extension can be evaluated from the equilibration scales above. One example of an equilibrated subsystem is illustrated by the case of a homogeneous interstitial melt in equilibrium with phenocryst rims. The *second part* comprises all phases (or fractions of phases) that are out of equilibrium with the first; for example, phenocryst cores, but also xenocrysts or even foreign magmatic liquids, as discussed in the examples above. In the following, the subsystem at chemical equilibrium will be designated as the *reactive magma*. Systems with strong chemical gradients (zoned interstitial glasses present; see above) can be treated as the sum of small equilibrated subsystems; that is, as the sum of small reactive magmas.

One important aspect of the concept is that the reactive magma is uniquely sensitive to physical processes or perturbations that affect the system and to their individual timescales. For a given system, there is no unique reactive magma. For example, let us consider an andesitic magma body evolving under closed-system steady-state pre-eruption conditions for 500 and 5000 years, and the same magma body decompressed from 200 MPa to the surface in 1 day and 1 month (Fig. 6). These four situations will generate different equilibration scales

and reactive magmas despite the fact that they concern the same body. The proposal that discrete episodes (each characterized by specific states of local equilibrium, hence specific reactive magma volumes and compositions) need to be distinguished in the lifetime of a magma chamber is now receiving support from geochronology. Zircon age data allow discrete stages of magma crystallization to be deconvoluted in long-lived silicic magmatic systems (e.g. Charlier *et al.*, 2005). Therefore, the reactive magma model appears consistent with temporal constraints on the evolution and dynamics of silicic magma bodies.

IMPLICATIONS FOR PHASE EQUILIBRIUM STUDIES

Chemical scaling of experiments

The recognition that chemical equilibrium in natural magmas is limited to a reactive subsystem requires phase equilibrium studies to be adapted. It is essential to approach closely the equilibrium state of the magma studied for a reliable determination of the pre-eruptive parameters. By analogy with the scaling of experiments in physics, phase equilibrium experiments need to be chemically scaled so that experimental and natural equilibrium states can be matched. To achieve this goal, specific experimental strategies and techniques need to be implemented. The choice of starting compositions is an obviously important point, although not the only one. In this respect, the use of synthetic analogues, rather than of natural rock starting materials, needs to be seriously considered. Synthetic oxide mixtures allow major and trace element compositions of starting products to be adjusted, as required for the chemical scaling of the experiments. With such mixtures, the textural and chemical complexities typical of bulk magmatic rocks would be absent. However, the use of natural rock starting materials has the decisive advantage of allowing direct comparison between experimental charges and eruption products. This comparison step is necessary for the precise determination of the pre-eruptive parameters (e.g. Martel *et al.*, 1999; Scaillet & Evans, 1999; Costa *et al.*, 2004). Therefore, natural rock starting materials of suitable composition, scaled to the local natural equilibrium state, have to be preferred.

Currently, there are essentially two groups of methods being developed to approach the equilibrium states of silicic magmas; that is, total and partial equilibrium experiments.

Total equilibrium experiments

Bulk-rock sample(s) chosen to be as close as possible to the composition of the reactive magma appropriate for pre-eruptive storage are used as starting materials (e.g. Martel *et al.*, 1999; Scaillet & Evans, 1999; Costa *et al.*, 2004). Thus, the chemical scaling of the experiments is entirely based on the rock selection. In practice, the sample is either fused to a glass or ground to a fine powder, to facilitate approach toward equilibrium. It should be noted that the use of glass does not necessarily mean acceptance of the idea that the studied magma body was once totally molten and that crystallization followed equilibrium crystallization. Glass is simply a convenient starting material to work with from the perspective of the attainment of equilibrium. In particular, the use of initially anhydrous starting glasses (e.g. Pichavant, 1987; Holtz *et al.*, 1992; Scaillet *et al.*, 1995; Martel *et al.*, 1999) greatly minimizes nucleation difficulties, especially for feldspars. This is because H_2O undersaturation and high degrees of undercooling initially prevail in the experiment, both conditions favouring crystal nucleation (Fenn, 1977). Crystallization experiments of this type generally yield homogeneous crystalline phases (Fig. 7a; Table 2), as crystal growth occurs under fixed conditions. Therefore, this method ensures a close approach to equilibrium. Reversals can be performed (two-stage crystallization–melting experiments, Holtz *et al.*, 1992) to check for the attainment of equilibrium. As the starting rock is assumed to

correspond to the composition of the reactive magma, the experimental and natural equilibrium states are identical (total equilibrium). However, the selection of the starting rock represents the main practical difficulty.

The critical importance of the selection of the starting composition may be illustrated on a ternary Qz–Ab–An phase diagram. Let us consider a simplified magma consisting of an interstitial melt (*l*) coexisting at equilibrium with plagioclase phenocrysts of composition *Pl* (Fig. 8a). The proportion of plagioclase phenocrysts is 17%, corresponding to the bulk composition *b*, which is also the composition of the reactive magma, as *l* and *Pl* are in equilibrium. Experiments performed on a starting composition identical to *b* at constant temperature (800°C), pressure and for two different melt H_2O contents (4 and 6 wt %) define two equilibrium liquid + plagioclase pairs (Fig. 8a), which bracket the composition of the interstitial melt and plagioclase phenocrysts. Experimental crystallinities (10 and 23%) also bracket the proportion of plagioclase phenocrysts in the magma. These results confirm that the natural *l* + *Pl* assemblage is an equilibrium assemblage, indicate that the natural equilibrium state is closely approached in the experiments and, consequently, allow the pre-eruptive melt H_2O concentration to be bracketed (H_2O melt = 4–6 wt %). It should be noted that, although a pre-eruptive temperature of 800°C was assumed, temperature (and also pressure) can be constrained in a way identical to that above for the melt H_2O content.
At the same temperature (800°C), for the same melt H_2O contents (4 and 6 wt % in melt), pressure and fO_2, experiments starting from composition *b1* yield two new equilibrium liquid + plagioclase pairs that differ from those obtained when starting from composition *b* (Fig. 8a and b). Composition *b1* is chosen so as to be enriched in plagioclase *Pl* relative to composition *b* (48% vs 17%), as would happen for a rock with cumulus plagioclase. As a result, plagioclase is more abundant in charges starting from the *b1* than from the *b* composition. Yet, the two new experimental pairs bracket the natural equilibrium *l* + *Pl* pair because the accumulated plagioclase has the equilibrium composition *Pl* (i.e. *l*, *b*, *b1* and *Pl* are collinear; Fig. 8b). Therefore, by using the starting composition *b1*, the same bracket on pre-eruptive melt H_2O content is obtained (i.e. 4–6 wt % H_2O). However, the fact that plagioclase proportions in experimental charges (33 and 53%) are higher than in the reactive magma *b* (17%) is an indication that *b1* grossly differs from the reactive magma composition. If now the experiments (at 800°C, for the same pressure and fO_2) start from a rock with xenocrystic plagioclase present (i.e. *b2*, obtained by adding 16% plagioclase Pl_x to *b*, Fig. 8c), the two experimental liquid + plagioclase pairs fail to bracket the natural *l* + *Pl* equilibrium pair. To approach *l*, melt H_2O concentrations >6 wt% would be needed, and, to approach *Pl*, < 4 wt% would be needed (Fig. 8c). In other words, the pre-eruptive melt H_2O content cannot be defined if *b2* is used as an experimental starting material. The definition of the pre-eruptive parameters therefore requires the use of starting compositions along the *l*–*Pl* tie-line or, more generally, of compositions lying within the multicomponent space defined by phases coexisting at equilibrium in the magma chamber.

Tests developed to check total equilibrium experiments involve comparison between phase proportions in addition to phase assemblages and compositions, in experimental and natural products. These tests can only be performed *a posteriori*, once the experimental programme has been completed. If the starting composition perfectly approximates the reactive magma, phase assemblages, compositions and proportions should be identical in both types of products (Appendix Fig. A1). As an example, the three experiments that are used to bracket the pre-eruptive conditions of the San Pedro dacite reservoir in Fig. 2 have crystal contents ranging between 24 and 37 wt %, whereas the erupted dacite contains 29 wt % phenocrysts (Costa *et al.*, 2004). In the case of the Mt. Pelée reservoir, the three experiments that best

define the pre-eruptive conditions (Fig. 2) have total proportions of crystals between 48 and 50 vol. %, identical to the proportion of phenocrysts in the starting materials (48 vol. %, Fig. A1). However, crystallinities in these experiments are higher than in the reactive magma by around 5 vol. % (Appendix, Fig. A1), indicating that the experimental starting materials (Martel *et al*., 1998, 1999) depart a little but significantly from the reactive magma composition (Appendix, Fig. A1; Table A1). Consequently, either the pre-eruptive melt H_2O concentration determined from these experiments is slightly underestimated (by <0·5 wt %) or, alternatively, the pre-eruptive temperature is slightly overestimated (by <25°C). In the same way, Blundy & Cashman (2001) have identified a mismatch between natural and experimental phase proportions, on one hand, and phase compositions, on the other hand, in experiments on the Mt. St. Helens dacite (Rutherford *et al*., 1985; Rutherford & Devine, 1988). One possible explanation would be the use, in these experiments, of a starting material less chemically evolved (i.e. poorer in SiO_2, richer in CaO) than the reactive magma appropriate for the 1980 Mt. St. Helens magma chamber.

Partial equilibrium experiments

As in the case of total equilibrium experiments, bulk-rock sample(s) representative of the magma studied are used. However, instead of glass or fine crystalline powder, coarse-grained starting materials obtained by light crushing are used as starting materials (Cottrell *et al*., 1999; Coombs *et al*., 2000; Hammer & Rutherford, 2002). In so doing, exposure of phenocryst cores to the melt is minimized and the reactive experimental system reduces (because of kinetic factors) to interstitial glass and phenocryst rims, phenocryst cores being excluded. The chemical scaling of the experiments is thus based on reaction kinetics, rather than on the selection of the appropriate rock composition as in the case of the total equilibrium approach.

The main characteristics of such experiments are that most crystalline phases are chemically heterogeneous (Fig. 7b), this heterogeneity being inherited from the starting material. Thus, total crystal–liquid equilibrium is not attained in the charge. In detail, the experimental results reflect the influence of non-intensive parameters such as the grain size of the starting powder, the experimental duration, and the heating and cooling rate. These latter parameters are imposed by practical laboratory constraints on equipment and run durations. Consequently, they cannot be scaled exactly to values in natural systems and, therefore, natural equilibrium states cannot be exactly reproduced. However, experimental melts reach steady-state compositions relatively rapidly. Partial equilibrium between melt and phenocryst rims is attained typically after durations of a few days (e.g. Cottrell *et al*., 1999; Coombs *et al*., 2000), although the definition of rim compositions may not be always straightforward (Fig. 7b). To allow a close approach to the natural equilibrium state, experiments of this type are usually kept within a narrow range of P–T–fH_2O–fO_2 conditions. Therefore, some *a priori* knowledge of these parameters (e.g. temperature from Fe–Ti oxides and melt H_2O content from the analysis of glass inclusions) is usually needed. Variations of melt and plagioclase rim compositions with experimental conditions provide a check of initial estimates of temperature and melt H_2O content, and allow the other parameters (e.g. pressure) to be determined (Cottrell *et al*., 1999; Coombs *et al*., 2000).

DISCUSSION

This overview illustrates the complementarity of experimental strategies and methods currently developed to approach equilibrium states in natural magmas. Total equilibrium experiments are to be preferred for systems with relatively large reactive magma volumes (i.e.

DICL systems). Partial equilibrium experiments are effective especially when information is already available on the conditions of natural equilibration, and they might be ideal to refine results from total equilibrium experiments. Combining the essential aspects of the two strategies above appears conceivably possible, and future studies in this direction are encouraged. Magmatic systems with small reactive magma volumes are especially challenging to handle (the reactive magma composition being difficult to define), and this should stimulate future developments. Some recent experimental studies illustrate the difficulty in reconstructing natural equilibrium states for systems with small reactive magma volumes such as, but not limited to, MD systems. For example, the fact that phenocryst assemblages are not reproduced in experimental charges despite variations and adjustments in P–T–fH$_2$O–fO$_2$ conditions (Berndt *et al.*, 2001; Gardner *et al.*, 2002; Harms *et al.*, 2004; Holtz *et al.*, 2005) is a strong indication of a compositional mismatch between the experimental starting material and the pre-eruptive reactive magma. It follows that, in the above studies, the pre-eruptive parameters cannot be constrained from an experimental approach only (Fig. 8). However, such results provide a conclusive demonstration of the lack of total equilibrium in the magmas studied, and have useful implications for the origin of crystals, either xenocrysts or phenocrysts (Gardner *et al.*, 2002; Harms *et al.*, 2004). A further illustration of the necessary sophistication of the phase equilibrium approach is provided by the Novarupta 1912 magma. This system shows several features indicating chemical disequilibrium, such as the presence of quartz xenocrysts in andesite, the occurrence of small-scale compositional zonation in magnetite, and Fe–Ti oxide pairs recording much higher temperatures than the majority of pairs (Hammer *et al.*, 2002). Experimental phase proportions reproduce phenocryst modes in the andesite, but at a temperature lower (930°C) than indicated by Fe–Ti oxides (960°C), suggesting thermal excursions driven by convection and mixing (Hammer *et al.*, 2002); yet tight constraints, notably on pressure and fH$_2$O, have been obtained from the careful experimental reconstruction of the natural local plagioclase–melt equilibrium state (Hammer *et al.*, 2002).

Finally, and although this paper has cautioned against the indiscriminate application of total equilibrium experiments to magmas, several characteristics of the total equilibrium approach are worth emphasis. (1) Information on the total equilibrium state of magmatic systems is useful as a reference end-member case, even if total equilibrium is not the rule in nature. This type of information is obtained from total equilibrium experiments, but is not accessible from partial equilibrium experiments. (2) As illustrated above, total equilibrium experiments are currently the only way to test for equilibrium (or the deviation from) in magmas (Fig. 2). (3) Total equilibrium experiments are the main source of data for the calibration of thermodynamic models for multicomponent melt and crystalline phases (Ghiorso & Sack, 1995). With the continuous development of such models, the reliable interpolation in the compositional space of equilibrium experimental data is within reach. Therefore, the calculation of crystal–liquid equilibria for compositions adjusted from bulk-rock compositions and representing reactive magma compositions (e.g. Table A1) will soon become possible.

CONCLUDING COMMENTS

The central point of this paper is the need to integrate better the specifics of natural equilibrium states in phase equilibrium experiments on silicic to intermediate magmas. The increasing use of experimental phase equilibria to precisely constrain intensive variables (P, T, fH$_2$O, fO$_2$) in igneous systems requires new standards to be set up. Experimental strategies and methods must adapt to the recognition that chemical equilibrium in natural magmas is limited to a reactive subsystem. For the petrologist, the detailed characterization of natural equilibrium states provides insights into magmatic timescales and the dynamics of magma

bodies. For the experimentalist, the laboratory reconstruction of the natural equilibrium states becomes a central objective, which guarantees a precise determination of the pre-eruptive parameters and a reliable application of the experimental data for the petrological monitoring of active volcanoes. Physical models of eruptions require a precise knowledge of parameters best constrained from experiments such as the depth of the storage region and the pre-eruptive volatile content of the magma. It is hoped that the challenging difficulties of handling systems with small reactive magma volumes will stimulate future experimental developments. Although one must caution against the uncritical application of total equilibrium experiments to magmas, it is nevertheless the case that these experiments continue to be of considerable theoretical and practical interest for modern igneous petrology.

APPENDIX

Worked example of calculation of the reactive magma composition

The calculation is performed for the andesitic magma body that forms the source of the recent (650 BP, 1902, 1929) andesitic eruptions from Mt. Pelée, Martinique, Lesser Antilles arc. Erupted andesites span a limited compositional range (58–65 wt % SiO_2, Fig. A1; Martel *et al*., 1998; Pichavant *et al*., 2002). Interstitial glasses are sub-homogeneous (Martel *et al*., 2000). The rocks contain a population of out-of-equilibrium phases including calcic plagioclase cores (Figs 1c and 2) and minor olivine and amphibole that comes from the crystallization of mafic magmas (Pichavant *et al*., 2002). Olivine and amphibole are present in low abundances and their influence is ignored in the calculation. The average of the three andesite starting materials (Martel *et al*., 1999) is taken as the bulk magma composition (column 1, Table A1; Fig. A1). Modal data (Martel, 1996) yields on average for the three rocks: matrix (52 vol. %), plagioclase (39 vol. %), orthopyroxene (7 vol. %) and magnetite (2 vol. %). Calcic plagioclase cores make up to 20 vol. % (Gourgaud *et al*., 1989; Martel, 1996) of the total plagioclase phenocryst content. For the purpose of the calculation, they are assumed to have a constant composition (An_{90}, Fig. 2; column 2, Table A1). The reactive magma composition is calculated by mass balance, subtracting from the bulk magma composition the contribution from the calcic plagioclase cores according to the equation oxide (wt %) in bulk magma = [oxide (wt %) in reactive magma]·[wt fraction of reactive magma] + [oxide (wt %) in plagioclase cores]·[wt fraction of plagioclase cores](A1)

where the weight fraction of reactive magma = 1 – the weight fraction of plagioclase cores. The latter is calculated from the modal data (see above), with volume per cent converted to weight per cent using standard density data for phenocryst and matrix (i.e. glass) phases. The calculated reactive magma is shifted to higher SiO_2 (by 1· 4 wt %, Table A1, column 3) and to lower volume per cent phenocrysts (by 4·4 vol. %) in comparison with the bulk magma composition (Fig. A1). The shift to lower Al_2O_3 and CaO contents should also be noted (Table A1, column 3).

ACKNOWLEDGEMENTS

Ideas developed in this paper have matured through years following discussions with Alain Weisbrod, Bill Brown, Jean-Louis Bourdier, Don Dingwell, Bernard Evans, Fabrice Gaillard and Steve Sparks, among others. We also acknowledge comments by Julia Hammer and several anonymous reviewers on previous versions. Constructive reviews by Jenni Barclay, Chris Hawkesworth and Malcolm Rutherford have substantially enriched the subject and improved its presentation. F.C. acknowledges a Ramon y Cajal Fellowship from the Spanish MEC.

REFERENCES

Allègre CJ, Minster JF. Quantitative models of trace element behaviour in magmatic processes. Earth and Planetary Science Letters (1978) 38:1–25

Anderson AT. Magma mixing: petrological processes and volcanological tool. Journal of Volcanology and Geothermal Research (1976) 1:3–33.

Annen C, Scaillet B, Sparks R. SJ. Thermal constraints on the emplacement rate of a large intrusive complex: the Manaslu leucogranite, Nepal Himalaya. Journal of Petrology (2006) 47:71–95.

Bacon CR. Magmatic inclusions in silicic and intermediate volcanic rocks. Journal of Geophysical Research (1986) 91:6091–6112.

Bacon CR, Druitt TH. Compositional evolution of the zoned calcalkaline magma chamber of Mount Mazama, Crater Lake, Oregon. Contributions to Mineralogy and Petrology (1988) 98:224–256.

Bacon CR, Hirschmann MM. Mg/Mn partitioning as a test for equilibrium between coexisting oxides. American Mineralogist (1988) 73:57–61.

Baschek G, Johannes W. The estimation of NaSi–CaAl interdiffusion rates in peristerite by homogenization experiments. European Journal of Mineralogy (1995) 7:295–307.

Bea F. Residence of REE, Y, Th and U in granites and crustal protoliths; implications for the chemistry of crustal melts. Journal of Petrology (1996a) 37:521–552.

Bea F. Controls on the trace element composition of crustal melts. Transactions of the Royal Society of Edinburgh: Earth Sciences (1996b) 87:33–41

Berndt J, Holtz F, Koepke J. Experimental constraints on storage conditions in the chemically zoned phonolitic magma chamber of the Laacher See volcano. Contributions to Mineralogy and Petrology (2001) 140:469–486.

Blundy J, Cashman K. Ascent-driven crystallization of dacite magmas at Mount St. Helens, 1980–1986. Contributions to Mineralogy and Petrology (2001) 140:631–650.

Bowen NL. The melting phenomena of the plagioclase feldspars. American Journal of Science, 4th Series (1913) 35:577–599.

Bowen NL. The ternary system: diopside–forsterite–silica. American Journal of Science, 4th Series (1914) 38:207–264.

Buddington AF, Lindsley DH. Iron–titanium oxide minerals and synthetic equivalents. Journal of Petrology (1964) 5:310–357.

Carmichael ISE, Nicholls J, Smith AL. Silica activity in igneous rocks. American Mineralogist (1970) 55:246–263.

Cashman KV. Textural constraints on the kinetics of crystallization of igneous rocks. In: Modern Methods of Igneous Petrology: Understanding Magmatic Processes. Mineralogical Society of America, Reviews in Mineralogy—Nicholls J, Russell JK, eds. (1990) 24:259–314.

Castro JM, Manga M, Martin MC. Vesiculation rates of obsidian domes inferred from H_2O concentration profiles. Geophysical Research Letters (2005) 32:L21307. doi:10.1029/2005GL024029.

Charlier B. LA, Wilson C. JN, Lowenstern JB, Blake S, Van Calsteren PW, Davidson JP. Magma generation at a large, hyperactive silicic volcano (Taupo, New Zealand) revealed by U–Th and U–Pb systematics in zircon. Journal of Petrology (2005) 46:3–32.

Cherniak DJ, Watson EB. Diffusion in zircon. In: Zircon. Mineralogical Society of America, Reviews in Mineralogy—Hanchar JM, Hoskin P. WO, eds. (2003) 53:113–143.

Cioni R, Civetta L, Marianelli P, Metrich N, Santacroce R, Sbrana A. Compositional layering and syn-eruptive mixing of a periodically refilled shallow magma chamber: the AD 79 plinian eruption of Vesuvius. Journal of Petrology (1995) 36:739–776.

Clemens JD, Wall VJ. Origin and crystallization of some peraluminous (S-type) granitic magmas. Canadian Mineralogist (1981) 19:111–131.

Clynne MA. A complex magma mixing origin for rocks erupted in 1915, Lassen Peak, California. Journal of Petrology (1999) 40:105–132.

Coombs ML, Gardner JE. Shallow-storage conditions for the rhyolite of the 1912 eruption at Novarupta, Alaska. Geology (2001) 29:775–778.

Coombs ML, Eichelberger JC, Rutherford MJ. Magma storage and mixing conditions for the 1953–1974 eruptions of Southwest Trident volcano, Katmai National Park, Alaska. Contributions to Mineralogy and Petrology (2000) 140:99–118.

Costa F, Chakraborty S. Decadal time gaps between mafic intrusion and silicic eruption obtained from chemical zoning patterns in olivine. Earth and Planetary Science Letters (2004) 227:517–530.

Costa F, Dungan M. Short time scales of magmatic assimilation from diffusion modelling of multiple elements in olivine. Geology (2005) 33:837–840.

Costa F, Singer BS. Evolution of Holocene dacite and compositionally zoned magma, Volcán San Pedro, Southern Volcanic Zone, Chile. Journal of Petrology (2002) 43:1571–1593.

Costa F, Chakraborty S, Dohmen R. Diffusion coupling between trace and major elements and a model for calculation of magma residence times using plagioclase. Geochimica et Cosmochimica Acta (2003) 67:2189–2200.

Costa F, Scaillet B, Pichavant M. Petrologic and phase equilibria constraints on the pre-eruption conditions of Holocene dacite from Volcán San Pedro (36°S, Chilean Andes) and the importance of sulfur in silicic subduction-related magmas. Journal of Petrology (2004) 45:855–881.

Cottrell E, Gardner JE, Rutherford MJ. Petrologic and experimental evidence for the movement and heating of the pre-eruptive Minoan rhyodacite (Santorini, Greece). Contributions to Mineralogy and Petrology (1999) 135:315–331.

Davidson JP, Tepley FJ. Recharge in volcanic systems: evidence from isotope profiles of phenocrysts. Science (1997) 275:826–829.

Devine JD, Rutherford MJ, Norton GE, Young SR. Magma storage region processes inferred from geochemistry of Fe–Ti oxides in andesitic magma, Soufrière Hills Volcano, Montserrat, W.I. Journal of Petrology (2003) 44:1375–1400.

Dimanov A, Jaoul O, Sautter V. Calcium self-diffusion in natural diopside single crystals. Geochimica et Cosmochimica Acta (1996) 60:4095–4106.

Dobran F, Neri A, Todesco M. Assessing the pyroclastic flow hazard at Vesuvius. Nature (1994) 367:551–554.

Druitt TH, Bacon CR. Petrology of the zoned calcalkaline magma chamber of Mount Mazama, Crater Lake, Oregon. Contributions to Mineralogy and Petrology (1989) 101:245–259.

Edwards B, Russell JK. Time scales of magmatic processes: new insights from dynamic models of magma assimilation. Geology (1998) 26:1103–1106.

Eggler DH, Burnham CW. Crystallization and fractionation trends in the system andesite–H_2O–CO_2–O_2 at pressures to 10 kbar. Geological Society of America Bulletin (1973) 84:2517–2532.

Eichelberger JC. Andesites in island arcs and continental margins: relationships to crustal evolution. Bulletin of Volcanology (1978) 41(4):480–500.

Eichelberger JC, Chertkoff DG, Dreher ST, Nye CJ. Magmas in collision: rethinking chemical zonation in silicic magmas. Geology (2000) 28:603–606.

Eichelberger JC, Izbekov PE, Browne BL. Bulk chemical trends at arc volcanoes are not liquid lines of descent. Lithos (2006) 87:135–154.

Feeley TC, Dungan MA. Compositional and dynamic controls on mafic–silicic magma interactions at continental arc volcanoes: evidence from Cordón El Guadal, Tatara–San Pedro complex, Chile. Journal of Petrology (1996) 37:1547–1577.

Fenn PM. The nucleation and growth of alkali feldspars from hydrous melts. Canadian Mineralogist (1977) 15:135–161.

Fougnot J, Pichavant M, Barbey P. Biotite resorption in dacite lavas from northeastern Algeria. European Journal of Mineralogy (1996) 8:625–638.

Freer R, Hauptman Z. An experimental study of magnetite–titanomagnetite interdiffusion. Physics of the Earth and Planetary Interiors (1978) 16:223–231.

Fuhrman ML, Lindsley DH. Ternary feldspar modelling and thermometry. American Mineralogist (1988) 73:201–215.

Gardner JE, Layer PW, Rutherford MJ. Phenocrysts versus xenocrysts in the youngest Toba Tuff: implications for the petrogenesis of 2800 km^3 of magma. Geology (2002) 30:347–350.

Gast PW. Trace element fractionation and the origin of the tholeiitic and alkaline magma types. Geochimica et Cosmochimica Acta (1968) 32:1057–1086.

Ghiorso M, Sack R. Chemical mass transfer in magmatic processes. IV. A revised and internally consistent thermodynamic model for the interpolation and extrapolation of liquid–solid equilibria in magmatic systems at elevated temperatures and pressures. Contributions to Mineralogy and Petrology (1995) 119:197–212.

Glazner AF, Bartley JM, Coleman DS, Gray W, Taylor RZ. Are plutons assembled over millions of years by amalgamation from small magma chambers? GSA Today (2004) 14:4–11.

Gourgaud A, Fichaut M, Joron J.-L. Magmatology of Mt. Pelée (Martinique, F.W.I.). I. Magma mixing and triggering of the 1902 and 1929 nuées ardentes. Journal of Volcanology and Geothermal Research (1989) 38:143–169.

Hammer JE, Rutherford MJ. An experimental study of the kinetics of decompression-induced crystallization silicic melt. Journal of Geophysical Research (2002) 107. doi:10.1029/2001JB00281.

Hammer JE, Rutherford MJ, Hildreth W. Magma storage prior to the 1912 eruption at Novarupta. Contributions to Mineralogy and Petrology (2002) 144:144–162.

Hammouda T, Pichavant M. Kinetics of melting of fluorphlogopite–quartz pairs at 1 atmosphere. European Journal of Mineralogy (1999) 11:637–653

Hammouda T, Pichavant M, Chaussidon M. Isotopic equilibration during partial melting: an experimental test on the behaviour of Sr. Earth and Planetary Science Letters (1996) 144:109–121.

Harford CJ, Sparks R. SJ, Fallick AE. Degassing at the Soufrière Hills volcano, Montserrat, recorded in matrix glass compositions. Journal of Petrology (2003) 44:1503–1523.

Harms E, Gardner JE, Schmincke H.-U. Phase equilibria of the Lower Laacher See tephra (east Eifel, Germany): constraints on pre-eruptive storage conditions of a phonolitic magma reservoir. Journal of Volcanology and Geothermal Research (2004) 134:125–138.

Hawkesworth C, George R, Turner S, Zellmer G. Time scales of magmatic processes. Earth and Planetary Science Letters (2004) 218:1–16.

Holtz F, Pichavant M, Barbey P, Johannes W. Effects of H_2O on liquidus phase relations in the haplogranite system at 2 and 5 kbar. American Mineralogist (1992) 77:1223–1241.

Holtz F, Sato H, Lewis J, Behrens H, Nakada S. Experimental petrology of the 1991–1995 Unzen dacite, Japan. Part I: phase relations, phase compositions and pre-eruptive conditions. Journal of Petrology (2005) 46:319–337.

Kerr RC. Convective crystal dissolution. Contributions to Mineralogy and Petrology (1995) 121:237–246.

Kirkpatrick RJ. Kinetics of crystallization of igneous rocks. In: Kinetics of Geochemical Processes. Mineralogical Society of America, Reviews in Mineralogy—Lasaga AC, Kirkpatrick RJ, eds. (1981) 8:321–398.

Knesel K, Davidson J, Duffield WA. Evolution of silicic magma through assimilation and subsequent recharge: evidence from Sr isotopes in sanidine phenocrysts, Taylor Creek rhyolite, NM. Journal of Petrology (1999) 40:773–786.

Kouchi A, Tsuchiyama A, Sunagawa I. Effect of stirring on crystallization kinetics of basalt: texture and element partitioning. Contributions to Mineralogy and Petrology (1986) 93:429–438.

Koyaguchi T, Kaneko K. Thermal evolution of silicic magma chambers after basalt replenishment. Transactions of the Royal Society of Edinburgh: Earth Sciences (2000) 91:47–60.

Kuno H. Petrology of Hakone volcano and the adjacent areas, Japan. Geological Society of America Bulletin (1950) 61:957–1014.

Kuo L-C, Kirkpatrick RJ. Kinetics of crystal dissolution in the system diopside–forsterite–silica. American Journal of Science (1985) 285:51–90.

Lasaga AC. Kinetic Theory in the Earth Sciences (1998) Princeton, NJ: Princeton University Press. 811.

La Tourette T, Wasserburg GJ. Mg diffusion in anorthite: implications for the formation of early solar system planetesimals. Earth and Planetary Science Letters (1998) 158:91–108.

Liang Y. Diffusive dissolution in ternary systems: analysis with applications to quartz and quartzite dissolution in molten silicates. Geochimica et Cosmochimica Acta (1999) 63:3983–3995.

Liang Y. Dissolution in molten silicates: effect of solid solution. Geochimica et Cosmochimica Acta (2000) 64:1617–1627.

Liang Y. Kinetics of crystal–melt reaction in partially molten silicates: 1. Grain scale processes. Geochemistry, Geophysics, Geosystems (2003) 4. paper number 2002GC000375.

Maaloe S, Wyllie PJ. Water content of a granite magma deduced from the sequence of crystallization determined experimentally under water-undersaturated conditions. Contributions to Mineralogy and Petrology (1975) 52:175–191.

Mandeville CW, Carey S, Sigurdsson H. Magma mixing, fractional crystallization and volatile degassing during the 1883 eruption of Krakatau volcano, Indonesia. Journal of Volcanology and Geothermal Research (1996) 74:243–274.

Manley CR, Bacon CR. Rhyolite thermobarometry and the shallowing of the magma reservoir, Coso volcanic field, California. Journal of Petrology (2000) 41:149–174.

Martel C. (1996) Conditions pré-éruptives et dégazage des magmas andésitiques de la Montagne Pelée (Martinique): étude pétrologique et expérimentale. PhD thesis, University of Orléans, 249 pp.

Martel C, Bureau H. *In situ* high-pressure and high-temperature bubble growth in silicic melts. Earth and Planetary Science Letters (2001) 191:115–127.

Martel C, Pichavant M, Bourdier J.-L, Traineau H, Holtz F, Scaillet B. Magma storage conditions and control of eruption regime in silicic volcanoes: experimental evidence from Mt. Pelée. Earth and Planetary Science Letters (1998) 156:89–99.

Martel C, Pichavant M, Holtz F, Scaillet B, Bourdier J.-L, Traineau H. Effects of fO_2 and H_2O on andesite phase relations between 2 and 4 kbar. Journal of Geophysical Research (1999) 104:29453–29470.

Martel C, Bourdier J.-L, Pichavant M, Traineau H. Textures, water content and degassing of silicic andesites from recent plinian and dome-forming eruptions at Mount Pelée volcano (Martinique, Lesser Antilles arc). Journal of Volcanology and Geothermal Research (2000) 96:191–206.

Mysen BO. Phase Diagrams for Ceramists, Volume 8 (1989) Columbus, OH: American Ceramic Society. 416.

Nakada S, Motomura Y. Petrology of the 1991–1995 eruption at Unzen: effusion pulsation and groundmass crystallization. Journal of Volcanology and Geothermal Research (1999) 89:173–196.

Nakamura M. Continuous mixing of crystal mush and replenished magma in the ongoing Unzen eruption. Geology (1995) 23:807–810.

Naney MT. Phase equilibria of rock-forming ferromagnesian silicates in granitic systems. American Journal of Science (1983) 283:993–1033.

Navon O, Chekhmir A, Lyakhovsky V. Bubble growth in highly viscous melts: theory, experiments, and autoexplosivity of dome lavas. Earth and Planetary Science Letters (1998) 160:763–776.

Nowak M, Behrens H. An experimental investigation on diffusion of water in haplogranitic melts. Contributions to Mineralogy and Petrology (1997) 126:365–376.

Pichavant M. The effect of boron and water on liquidus phase relations in the haplogranite system at 1 kbar. American Mineralogist (1987) 72:1056–1070.

Pichavant M, Martel C, Bourdier J.-L, Scaillet B. Physical conditions, structure and dynamics of a zoned magma chamber: Mt. Pelée (Martinique, Lesser Antilles Arc). Journal of Geophysical Research (2002) 107. doi:10.1029/2001JB000315.

Pons J, Barbey P, Nachit H, Burg J.-P. Development of igneous layering during growth of pluton: the Tarçouate laccolith (Morocco). Tectonophysics (2006) 413:271–286.

Poussineau S. (2005) Dynamique des magmas andésitiques: approche expérimentale et pétrostructurale; application à la Soufrière de Guadeloupe et à la Montagne Pelée. PhD thesis, University of Orléans, 295 pp.

Rutherford MJ, Devine JD. The May 18, 1980, eruption of Mount St. Helens 3. Stability and chemistry of amphibole in the magma chamber. Journal of Geophysical Research (1988) 93:11949–11959.

Rutherford MJ, Hill PM. Magma ascent rates from amphibole breakdown: an experimental study applied to the 1980–1986 Mount St. Helens eruptions. Journal of Geophysical Research (1993) 98:19667–19685.

Rutherford MJ, Sigurdsson H, Carey S, Davis A. The May 18, 1980, eruption of Mount St. Helens 1. Melt composition and experimental phase equilibria. Journal of Geophysical Research (1985) 90:2929–2947.

Scaillet B, Evans B. The 15 June 1991 eruption of Mount Pinatubo. I. Phase equilibria and pre-eruption P–T–$f$$H_2O$–$f$$O_2$ conditions of the dacite magma. Journal of Petrology (1999) 40:381–411.

Scaillet B, Pichavant M. Experimental constraints on volatile abundances in arc magmas and their implications for degassing processes. In: Volcanic Degassing. Geological Society, London, Special Publications—Oppenheimer C, Pyle DM, Barclay J, eds. (2003) 213:23–52.

Scaillet B, Pichavant M, Roux J. Experimental crystallization of leucogranite magmas. Journal of Petrology (1995) 36:663–705.

Schairer JF. Melting relations of the common rock-forming oxides. Journal of the American Ceramic Society (1957) 40:215–235.

Schmidt MW. Amphibole composition in tonalite as a function of pressure: an experimental calibration of the Al-in-hornblende barometer. Contributions to Mineralogy and Petrology (1992) 110:304–310.

Schmitz MD, Smith I. EM. The petrology of the Rotoiti eruption sequence, Taupo volcanic zone: an example of fractionation and mixing in a rhyolitic system. Journal of Petrology (2004) 45:2045–2066.

Singer BS, Dungan MA, Layne GD. Textures and Sr, Ba, Mg, Fe, K, and Ti compositional profiles in volcanic plagioclase: clues to the dynamics of calc-alkaline magma chambers. American Mineralogist (1995) 80:776–798.

Smith RL. Ash-flow magmatism. In: Ash-Flow Tuffs—Chapin CE, Elston WE, eds. (1979) Boulder, CO: Geological Society of America. 5–42.

Thompson JB Jr. Local equilibrium in metasomatic processes. In: Researches in Geochemistry—Abelson PH, ed. (1959) London: Wiley. 427–457.

Tsuchiyama A. Partial melting kinetics of plagioclase–diopside pairs. Contributions to Mineralogy and Petrology (1985) 91:12–23.

Watson EB. Diffusion in volatile-bearing magmas. In: Volatiles in Magmas. Mineralogical Society of America, Reviews in Mineralogy—Carroll MR, Holloway JR, eds. (1994) 30:371–411.

Wörner G, Schmincke H.-U. Mineralogical and chemical zonation of the Laacher See Tephra Sequence (East Eifel, W. Germany). Journal of Petrology (1984) 25:805–835.

Yoder HS, Jr. Albite–anorthite–quartz–water at 5 kbar. Carnegie Institution of Washington Yearbook (1968) 66:477–478.

Young DA. N. L. Bowen and Crystallization–Differentiation: the Evolution of a Theory (1998) Washington, DC: Mineralogical Society of America. 276.

Zhang Y, Walker D, Lesher CE. Diffusive crystal dissolution. Contributions to Mineralogy and Petrology (1989) 102:492–513.

FIGURES

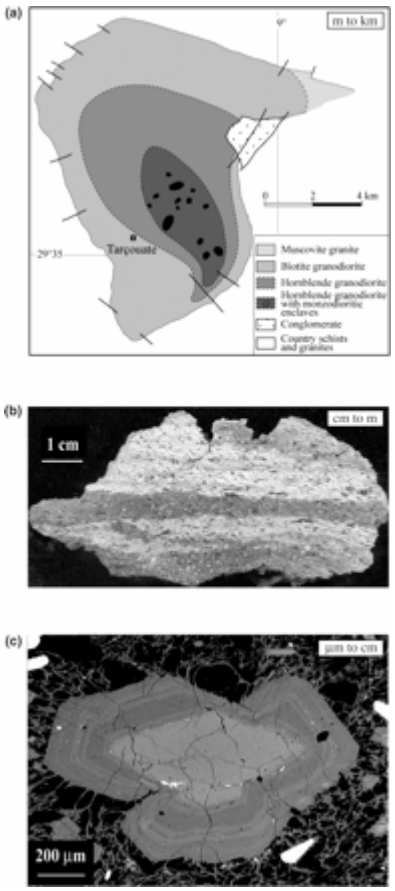

Fig. 1. Examples of chemical heterogeneities at various scales in silicic to intermediate magmas. (a) Compositional and mineralogical zonation at scales up to kilometre scale illustrated by the Tarçouate zoned pluton, Morocco (modified after Pons *et al*., 2006); (b) banded pumiceous rock from the AD 1440 eruption of Soufrière, Guadeloupe, records mixing between silicic andesite and basaltic andesite magmas at centimetre to decimetre scales (Poussineau, 2005); (c) compositional heterogeneties at scales as low as ≤1 µm revealed by back-scattered electron imaging of plagioclase phenocryst from the P1 eruption of Mt. Pelée, Martinique (Martel *et al*., 1998; Pichavant *et al*., 2002; see also Fig. 2).

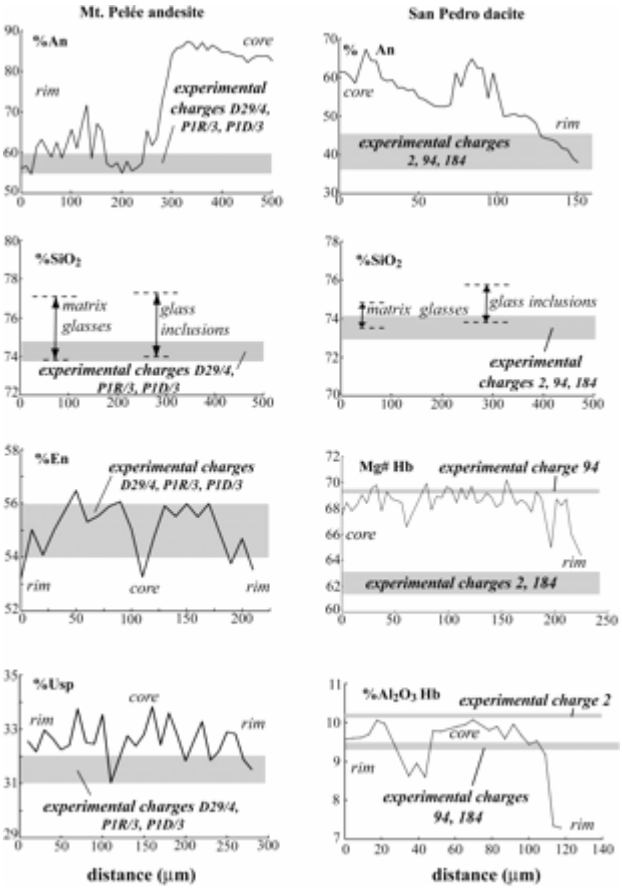

Fig. 2. Testing for chemical equilibrium in two intermediate arc magmas. Comparison between phenocryst and glass compositions in Mt. Pelée and Volcán San Pedro eruptive products and in selected equilibrium experimental charges. Experimental details for Mt. Pelée charges D29/4, P1R/3 and P1D/3 have been given by Martel *et al*. (1999) and for San Pedro charges 2, 94 and 184 by Costa *et al*. (2004). In both cases, equilibrium charges simultaneously reproduce glass SiO2 contents and compositions of the main magmatic phenocrysts (Mt. Pelée: plagioclase, orthopyroxene, magnetite; San Pedro: plagioclase, hornblende), with the exception of plagioclase cores. It should be noted that the composition of hornblende in the San Pedro dacite is bracketed, rather than exactly reproduced, by the experiments. %An, proportion of anorthite in plagioclase; % SiO2, wt % SiO2 in glass; %En, proportion of enstatite in orthopyroxene; %Usp, proportion of ulvöspinel in magnetite; Mg# Hb, Mg/(Mg + Fe_{tot}) in hornblende; %Al_2O_3 Hb, wt % Al_2O_3 in hornblende.

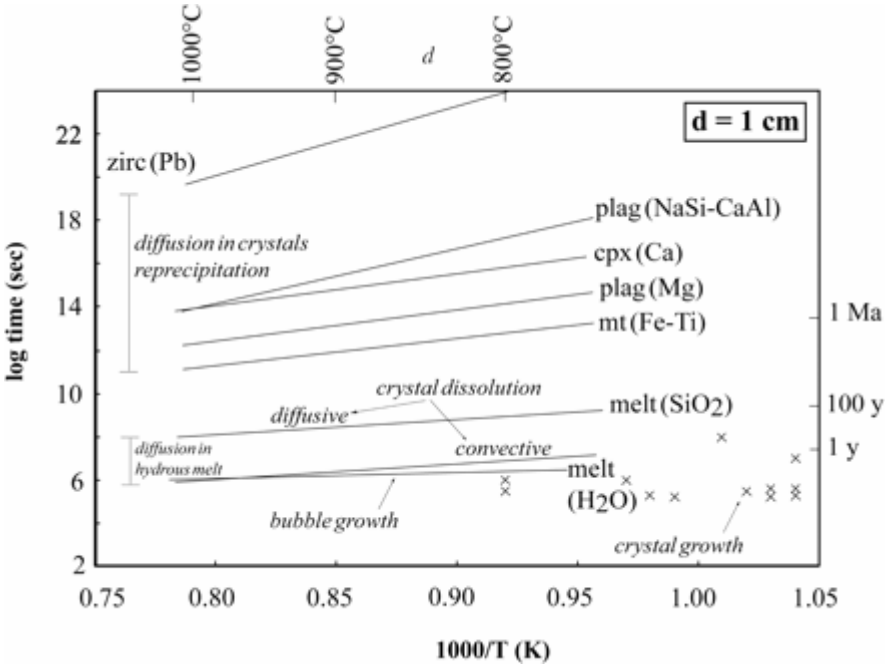

Fig. 3 Timescales of equilibration mechanisms in silicic to intermediate magmas normalized to a common distance of 1 cm and plotted as a function of reciprocal temperature (Edwards & Russell, 1998). Timescales of diffusive equilibration in representative crystals and in hydrous melt are calculated using the relation $t = x^2/D$, where x is the distance (1 cm) and D is the diffusion coefficient. Diffusion coefficients for Pb in zircon (zirc) from Cherniak & Watson (2003), for NaSi–CaAl exchange in plagioclase (plag) from Baschek & Johannes (1995), for Mg in plagioclase from La Tourette & Wasserburg (1998), for Ca in diopside (cpx) from Dimanov *et al*. (1996), for Fe–Ti in magnetite (mt) from Freer & Hauptman (1978), and for SiO_2 and H_2O in hydrous melt from Watson (1994) and Nowak & Behrens (1997), respectively. Timescales of crystallization are constrained by crystal growth rate data (x) for quartz, alkali feldspar and plagioclase in hydrous silicic melts (Cashman, 1990). Timescales for bubble growth are approximated from H_2O diffusion (Nowak & Behrens, 1997). The timescale for diffusive crystal (quartz) dissolution is approximated from SiO_2 diffusion in hydrous melt (Watson, 1994). The timescale for convective quartz dissolution is calculated following Kerr (1995). The boundary layer thickness for free convection (h_c) is obtained from equations (8) and (11) of Kerr (1995), taking a density difference of 0·1 g/cm^3 between the interfacial melt and the far-field melt, a diameter of 1 cm for the dissolving spherical crystal, a diffusivity of SiO_2 in hydrous melt from Watson (1994) and a melt viscosity of $10^{3·7}$ Pa s (Pichavant *et al*., 2002). Then, the convective dissolution rate is calculated from equation (6) of Kerr (1995), and assumed to be constant with temperature. (See text for details and explanation.)

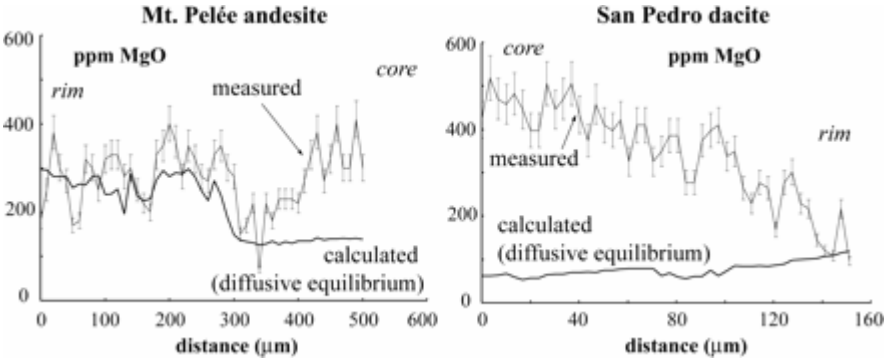

Fig. 4. Electron microprobe profiles for a trace element (Mg) in the same plagioclase phenocrysts as in Fig. 2. Measured concentrations are plotted with error bars. For comparison, Mg concentrations calculated assuming diffusive equilibrium in each crystal are shown (black continuous curves). These are calculated following the procedures detailed by Costa *et al*. (2003), assuming that crystal–liquid equilibrium is established at the edge of each crystal. In the Mt. Pelée phenocryst, the entire rim zone and the outer part of the core are in diffusive equilibrium. Therefore, Mg is homogeneously distributed in a substantial part of the crystal whereas strong variations in An content persist (Fig. 2). In contrast, in the Volcán San Pedro phenocryst, equilibrium Mg concentrations are restricted to the outer rim of the crystal. MgO concentrations systematically increase from rim to core, closely following variations in An content (Fig. 2).

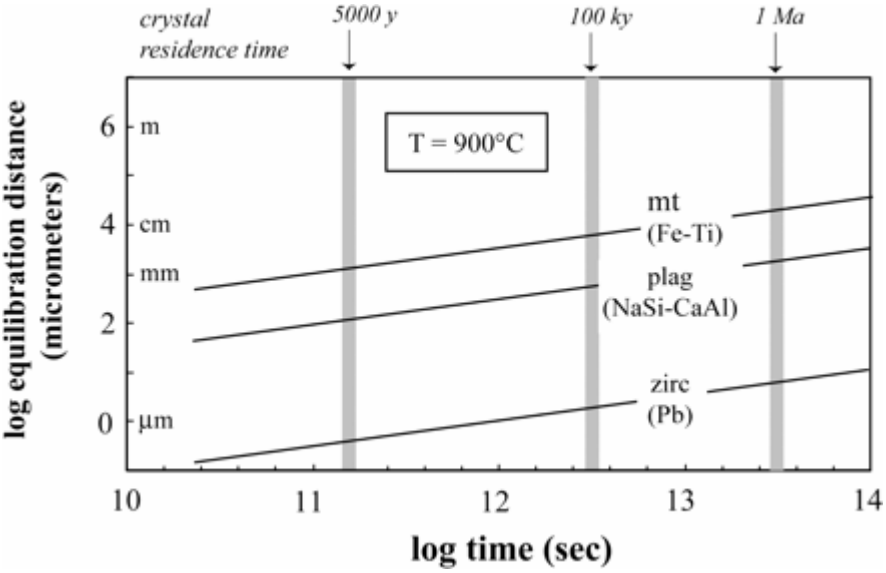

Fig. 5. Equilibration regime rate-controlled by diffusion in crystals. Equilibration distances (x) calculated as a function of time (t) at 900°C for magnetite (mt) plagioclase (plag) and zircon (zirc) using the relation $x = (Dt)^{1/2}$, with diffusion coefficients as in Fig. 3. (See text for details and explanation.)

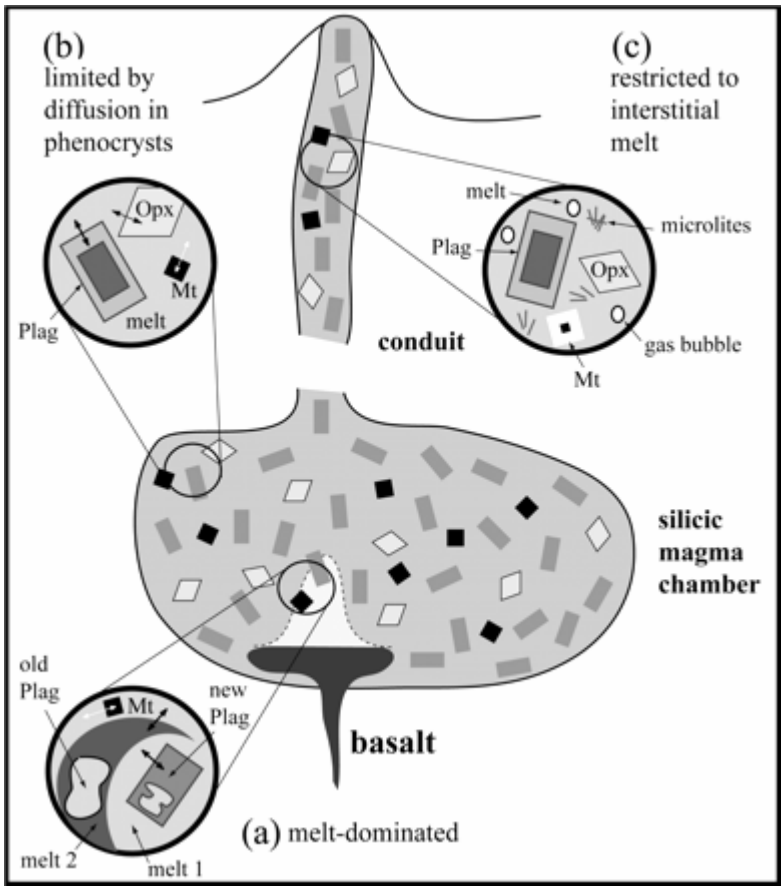

Fig. 6. Illustration of equilibration regimes discussed in this paper. (a) Pre-eruptive equilibration regime controlled by melt-dominated (MD) reaction mechanisms (convective mixing and chemical diffusion between melt 1 and melt 2, dissolution of old plagioclase, crystallization of new plagioclase). (b) Pre-eruptive equilibration regime limited by diffusive flux in crystals. Chemical equilibration, indicated by double-ended arrows, is achieved between homogeneous interstitial melt, orthopyroxene, magnetite and plagioclase rim. (c) Syn-eruptive, ascent-related, equilibration regime essentially involving reactions in the interstitial melt (crystallization of microlites, vesiculation of gas bubbles). Depending on magma ascent rates, chemical equilibration may be achieved between melt and the outer rims of some phenocrysts (magnetite, but not orthopyroxene and plagioclase), as indicated by the white rim around magnetite. Plag, plagioclase; Opx, orthopyroxene; Mt, magnetite. (See text for details and explanation.)

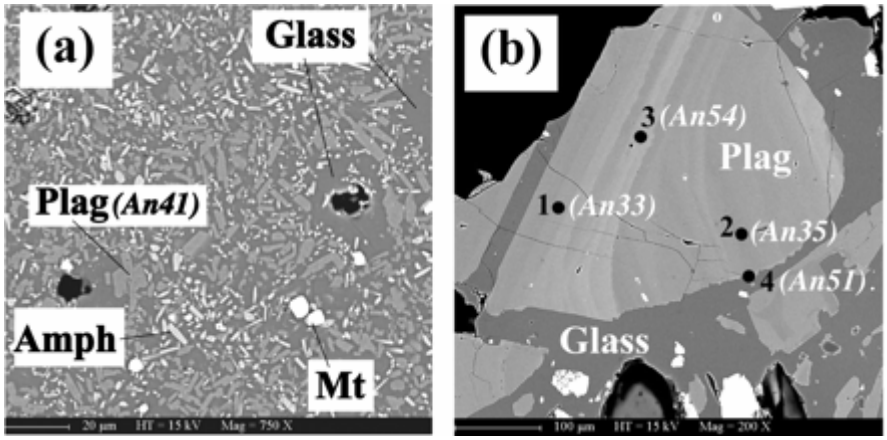

Fig. 7. Scanning electron microphotographs of experiments on the 1991 Mt. Pinatubo dacite magma. Experiments have been performed under nearly identical conditions (217–221 MPa, 778–785°C, 470–502 h, Scaillet & Evans, 1999) using two different types of starting materials: (a) total equilibrium experiment PIN 8 using dacite glass starting material; (b) partial equilibrium experiment PIN 4 using coarse-grained dacite starting material. The change in scale and the textural and compositional differences between (a) and (b) should be noted. In (a) crystals are chemically homogeneous, whereas in (b) they are heterogeneous (Table 2). In (b) the numbered spots 1–4 refer to the analyses in Table 1. Plag, plagioclase; Amph, amphibole; Mt, magnetite.

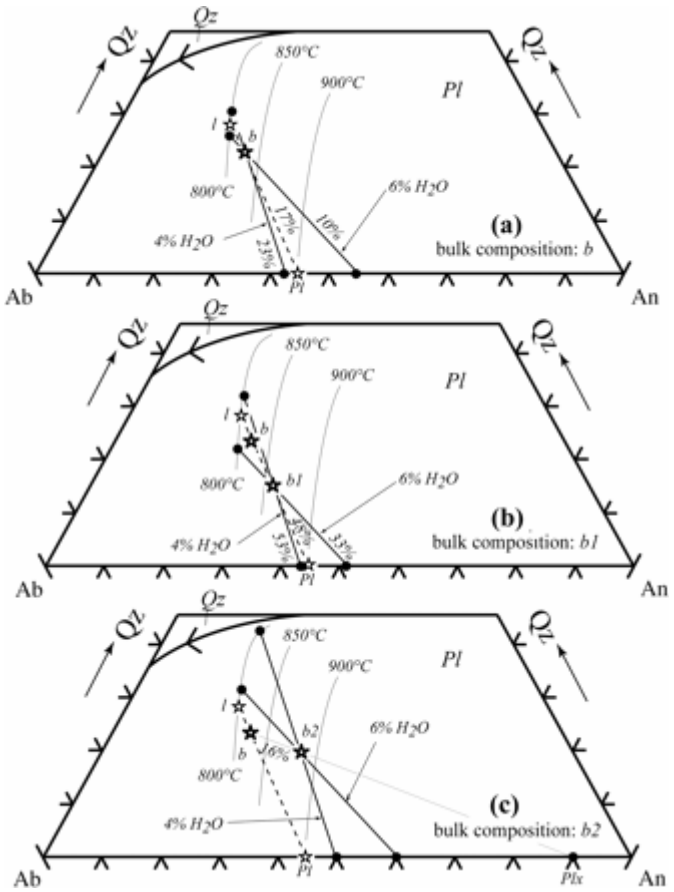

Fig. 8. Influence of starting bulk composition on plagioclase–liquid phase equilibria in the quartz–albite–anorthite system, drawn after Yoder (1968). Experiments are designed to bracket the pre-eruptive melt H_2O concentration in a simplified magma of bulk composition

b. Magma *b* is assumed to consist of a mixture of interstitial melt *l* at equilibrium with plagioclase phenocrysts of composition *Pl* (equilibrium compositions *l* and *Pl* are connected by a dashed line). Experiments are performed at constant temperature (800°C), pressure and fO_2. Tie-lines connecting equilibrium experimental compositions (large dots) are shown as black continuous lines. Their slopes (identical in the three diagrams) depend only on the H_2O concentration of the melt (either 4 or 6 wt %). Italic numbers are proportions of plagioclase determined from the lever rule. Qz, quartz primary phase field; Pl, plagioclase primary phase field. (a) Experiments with starting composition *b*. Both the equilibrium melt *l* and plagioclase compositions *Pl* are bracketed by the two experimental charges with 4 and 6 wt % H_2O in the melt. It should be noted that the proportion of plagioclase phenocrysts in magma *b* (17%) is also bracketed. (b) Experiments with starting composition *b1*. The equilibrium melt *l* and plagioclase compositions *Pl* are bracketed by the two experimental charges with 4 and 6 wt % H_2O in the melt but proportions of plagioclase in the two experiments are higher than in magma *b*. (c) experiments with starting composition *b2*. No experiment can simultaneously bracket the equilibrium melt *l* and plagioclase compositions *Pl*.

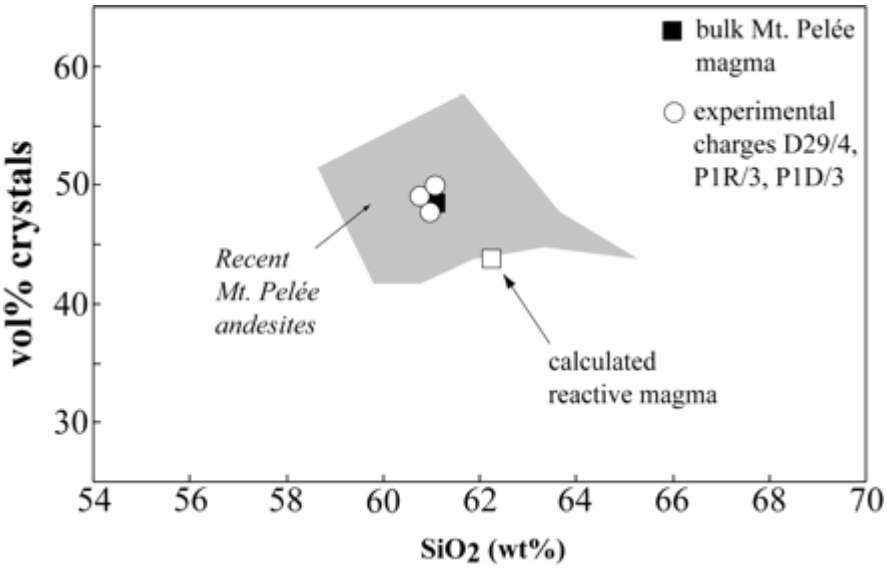

Fig. A1. Crystallinities and bulk SiO_2 compositions in natural andesites and experimental charges from Mt. Pelée. Data for the andesites (grey field) are from Gourgaud *et al*. (1989) and Martel (1996), with crystallinities refering to phenocryst contents determined by point counting. The bulk Mt. Pelée magma is the average of three natural andesites chosen as starting materials for the experiments of Martel *et al*. (1998, 1999). Three experimental charges are plotted; these have been selected to closely approach the pre-eruptive magma storage conditions (Fig. 2). SiO_2 concentrations and crystallinities in these three experimental charges (Martel *et al*., 1999) and in the bulk Mt. Pelée magma are almost identical. In comparison, the reactive magma calculated for the Mt. Pelée reservoir (see Appendix) is shifted towards higher SiO_2 and lower phenocryst contents. Therefore, the experimental starting materials used (Martel *et al*., 1998, 1999) do not exactly match the reactive magma composition.

TABLES

Table 1: Definition of equilibrium states used in this paper

Equilibrium state	Definition
Total	Chemical equilibrium for all chemical components and phases present in the system
Local	Chemical equilibrium for all chemical components and phases; for certain phases present in the system, only a limited fraction is equilibrated; the equilibration scale is a measure of the spatial extent of the equilibrated fraction
Partial	Chemical equilibrium only for some chemical components and phases, or a fraction of, present in the system

Table 2: Electron microprobe data for experimental charges shown in Fig. 7

Exp. no.:	PIN 8*			PIN 4*						
Phase	plag.	amph.	mt.	plag.				amph.		
Analysis no.:	*n* = 3	*n* = 5	*n* = 5	1	2	3	4	5	6	7
SiO_2	58·5(85)	48·7(1.14)	0·24(11)	59·8	60·4	55·0	55·1	47·5	48·6	51·8
TiO_2	0·07(7)	1·11(18)	1·96(10)	0·05	0·00	0·01	0·06	0·98	0·92	0·46
Al_2O_3	25·6(68)	9·39(26)	2·20(5)	24·8	25·2	28·6	27·7	8·23	7·21	5·06
Cr_2O_3	0·01(1)	0·06(4)	0·03(5)	0·00	0·00	0·00	0·00	0·00	0·00	0·00
FeO	0·70(16)	10·0(63)	85·2(58)	0·13	0·00	0·19	0·44	13·51	12·88	8·32
MnO	0·06(6)	0·42(12)	0·66(13)	0·00	0·00	0·00	0·00	0·44	0·21	0·45
NiO	0·04(6)	0·03(8)	0·14(8)	0·00	0·00	0·00	0·00	0·03	0·12	0·00
MgO	0·13(16)	14·9(52)	1·86(5)	0·00	0·02	0·04	0·02	14·9	15·1	18·4
CaO	8·23(57)	10·9(32)	0·20(5)	6·67	7·31	11·02	10·8	10·4	10·1	11·3
Na_2O	6·27(31)	1·69(9)	0·04(4)	7·24	7·20	5·01	5·53	1·39	1·29	0·93
K_2O	0·30(1)	0·37(6)	0·04(3)	0·33	0·29	0·15	0·17	0·28	0·20	0·13
Total	99·9	97·6	92·6	99·0	100·4	100·0	99·8	97·7	96·6	96·9
An	41·3	—	—		33·1	35·3	54·4	51·4	—	— —

*See Scaillet & Evans (1999) for experimental conditions.

For PIN 8, the data are average values, *n* being the number of analyses. Standard deviations are shown in parentheses in terms of least unit cited. For PIN 4, analyses 1–4 are located in Fig. 7. An = 100 x Ca/(Ca + Na + K) atomic. plag., plagioclase; amph., amphibole; mt., magnetite.

Table A1: Calculation of the reactive magma composition for the Mt. Pelée reservoir (see Appendix)

	1 bulk magma	2 plagioclase core	3 reactive magma	4* relative difference (%)
SiO_2	60·94	45·8	61·77	1·4
TiO_2	0·45	0·02	0·47	4·4
Al_2O_3	17·56	34·6	16·62	–5·4
FeO	5·98	0·51	6·28	5·0
MnO	0·18	0·04	0·19	5·6
MgO	2·22	0·09	2·34	5·4
CaO	6·18	18·0	5·53	–10·5
Na_2O	3·5	1·08	3·63	3·7
K_2O	1·02	0	1·08	5·9
Total	98·03	100·1	97·91	–0·1

*Calculated as [(oxide in bulk magma – oxide in reactive magma)/(oxide in bulk magma)] x 100.